Experimentally established correlation of friction surfacing process temperature and deposit geometry

Kallien, Zina; Rath, Lars; Roos, Arne; Klusemann, Benjamin

Published in:
Surface and Coatings Technology

DOI:
10.1016/j.surfcoat.2020.126040

Publication date:
2020

Document Version
Publisher's PDF, also known as Version of record

Surface & Coatings Technology 397 (2020) 126040

Contents lists available at ScienceDirect

Surface & Coatings Technology

journal homepage: www.elsevier.com/locate/surfcoat

Experimentally established correlation of friction surfacing process temperature and deposit geometry

Zina Kallien[a,*], Lars Rath[a], Arne Roos[a], Benjamin Klusemann[a,b]

[a] Helmholtz-Zentrum Geesthacht, Institute of Materials Research, Materials Mechanics, Solid State Joining Processes, Max-Planck-Straße 1, 21502 Geesthacht, Germany
[b] Leuphana University of Lüneburg, Institute of Product and Process Innovation, Universitätsallee 1, 21335 Lüneburg, Germany

ARTICLE INFO

Keywords:
Friction surfacing
Deposit geometry
Temperature
Dissimilar aluminum alloys

ABSTRACT

Friction surfacing (FS), a solid-state joining process, is a coating technology for metallic materials. Friction and plastic deformation enable the deposition of a consumable material on a substrate below the melting temperature. Process temperatures are an important factor determining the quality and geometry of the deposit. A detailed experimental study of the process temperatures during FS of dissimilar aluminum alloys is performed. The process temperature profiles for varied process parameters, i.e. axial force, rotational speed and travel speed as well as process environment, are investigated. The results show that axial process force and rotational speed are the dominant process parameters affecting the temperatures during the FS process. Additionally, backing material and substrate thickness have significant impact on the process temperatures. The correlation of deposit geometry with process temperature shows thinner and slightly wider deposits for increasing process temperatures. This finding pronounces the importance of the temperature for the friction surfacing process with regard to geometry of the resulting deposit.

1. Introduction

The design of lightweight and perdurable structures demand highly developed processing technologies. Solid-state joining processes are an alternative to conventional fusion-based joining techniques [1]. Especially the surface engineering has gained importance since phenomena like wear, corrosion or fatigue happen on the surface and result in failure of a component [2]. Friction surfacing (FS) is a solid-state coating technology for metallic materials allowing the joining of similar and dissimilar material combinations. Due to the solid-state nature of the process, the lower heat input during FS compared to fusion-based processes leads to a reduced heat affected zone (HAZ) and prevents large distortion parts [3]. The thermo-mechanical input by FS on the material results in a fine grained microstructure enabled by dynamic recrystallization. The process is environmentally friendly and does not have high demands on process environment because shielding gas and cooling are not necessarily needed.

The FS process starts with the positioning of the consumable stud material above the substrate. When the rotation of the stud has started, axial force is applied and the stud is pressed onto the substrate. Due to friction, heat is generated and the tip of the stud plasticizes. The plasticized material is pressed to the outside and the process-typical flash is formed at the stud. The relative movement between stud and substrate starts at a defined travel speed and a layer of the quasi-liquid stud material is deposited on the substrate. The process ends with stopping the relative movement between stud and substrate and the retraction of the remaining stud material. Being a discontinuous process, the stud's length is a limiting factor with regard to the length of the coating and the amount of deposited material. Since the coating layer has some unbonded regions outside the main bonding area [4], further processing might be necessary. The possibility to deposit multiple layers underlines that the FS process also offers potential for additive manufacturing [5–7]. Moreover, the process can be applied as repair technology [8]. As Huang et al. [9] showed, sound bondings are even achievable for dissimilar material combinations, i.e. aluminum and titanium via a hybrid FS process assisted by friction stir welding (FSW). In order to use the great potential of FS, a fundamental understanding of the complex relation of material properties, process parameters, process environment and temperature as well as changes in the material, geometry and quality of the joint has to be achieved.

The main process parameters affecting the resulting joint are axial force, rotational speed and travel speed. As discussed in detail in the review article by Gandra et al. [10], these process parameters have significant influence on the geometry of the deposit, which is mainly characterized by deposit thickness and width. Apart from the duration of the process, the amount of deposited material can be used to evaluate

* Corresponding author.
E-mail address: zina.kallien@hzg.de (Z. Kallien).

https://doi.org/10.1016/j.surfcoat.2020.126040
Received 1 April 2020; Received in revised form 2 June 2020; Accepted 5 June 2020
Available online 10 June 2020

the process efficiency [11]. Not only the deposit geometry is affected by the process parameters, but also the mechanical performance of the joint. For example, increased travel speeds result in better bonding properties of the coating to the substrate [12,13]. Govardhan et al. [14] observed that an increased travel speed results in a decreased tensile strength and increased shear strength. Furthermore, Rafi et al. [12] mentioned that the rotational speed does not seem to affect the bond strength. Since higher rotational speeds introduce more heat, a deeper HAZ was found where higher travel speeds lead to a reduced size of HAZ. From this finding the importance of process parameter selection for the heat input is visible. There are first studies [15–17], which discuss the influence of process parameters, i.e. axial force rotational speed and travel speed, on the temperature development during FS, however, a comprehensive study providing a clear correlation to the deposit geometry is missing.

The temperature evolution during FS is characterized by a sudden increase in temperature when consumable and substrate material get in contact [18,19]. The temperature at the materials' interface reaches a stable value below the melting point, i.e. maximal 80% of it [20], and the system becomes steady state [18]. During the process, the highest temperatures can be found in the shear zone between the rotating stud and the already deposited material [21]. The steady state during the process is a result of viscous heat dissipation during plastic deformation, where the process duration is short enough to be approximated as adiabatic [19]. The thermal loads and severe plastic deformation lead to microstructural changes in both substrate and consumable stud [19], i.e. typically strong grain refinement due to dynamic recrystallization is observed [22]. Since the required energy input for the process is strongly dependent on the temperature-dependent material properties [21], the choice of materials to be welded is fundamental for the selection of the process parameters. For constant process parameters and systematic variation of Si content in AA6060 stud material, Ehrich et al. [23] observed that AA6060 stud material with higher Si content results in lower process temperature than AA6060 stud material. Furthermore, the deposition efficiency as well as the energy input per volume was found to correlate with the dimensions of the deposited material. At constant process parameters, deposits of a smaller volume resulted in a lower efficiency and high energies whereas deposits of a larger volume resulted in high efficiency and low energies [23].

Krohn et al. [24] found that external cooling influences deposition width. This finding shows that the deposition geometry is not simply dependent on the choice of process parameters but in particular on the temperature evolution during FS. A recent study by Isupov et al. [25] mentioned deposit thickness depending on the distribution of the temperature field.

The focus of the present study is the systematic investigation of the relation between FS parameters, i.e. process parameters, substrate thickness as well as process environment, and the resulting process temperature. A special focus lies on the correlation between process temperature and deposition geometry. Especially the understanding of the correlation between deposit geometry and temperature is of fundamental interest.

2. Materials and methods

In this study, AA 5083 H112 was used as consumable stud material (20 mm diameter, 125 mm length) to be deposited on AA 7050 T7451 substrates (300 mm length, 100 mm width, 8 mm to 20 mm thickness). In order to perform temperature measurements as close as possible to the process zone, eight holes were drilled from the backside into the substrate until 0.5 mm below the substrate's surface. The holes of 1 mm in diameter were evenly distributed from the center of the substrate every 5 mm, as schematically shown in Fig. 1. Each hole was filled with thermal paste and one thermocouple (Type K) was positioned as close as possible to the substrate surface. The temperatures were recorded at a frequency of 50 Hz. The distribution of the measurement points allows the analysis of the temperature evolution during FS along layer width from advancing to retreating side. For the process parameter investigation, an AA 7050 backing plate (300 mm length, 130 mm width, 8 mm thickness) was used between substrate and machine table as well as a studholder of X 37 tool steel. For the investigation of the process environment, the backing plate was varied to AA 7050 (300 mm length, 100 mm width, 12.5 mm thickness) and Ti64 (300 mm length, 100 mm width, 10.2 mm thickness) as well as the studholder material from X 37 tool steel to AA 6060.

The experiments are performed on a custom-designed friction welding system (working area of 0.5 m × 1.5 m) by Henry Loitz Robotik, Germany, allowing maximum forces of 60 kN, maximum rotational speed of 6000 rpm and maximum torque of 200 Nm. The FS deposition process was initiated 70 mm before the temperature measurement points and stopped 70 mm behind the measurement points, resulting in 140 mm of total welding distance. The positioning of the stud's center above the substrate's centerline was constant over all experiments, see Fig. 1.

In order to analyze the deposit, the specimens were cut, ground and polished. Optical analysis and imaging of the deposited structures was performed with a VHX-6000 digital microscope by Keyence, Germany. The deposit thickness is determined from the average of eight thickness values measured in equispaced distances of 2 mm along the cross section of the deposit. The deposit width is measured at not less than seven points in the cross section at equispaced distances of 0.2 mm. The positioning of the deposit is exemplarily shown in Fig. 2. As can be seen, the centerline of the deposit does not correspond to the centerline of the substrate since the stud has the tendency to be deflected to the advancing side during the process. Therefore, the position of the measurement points in relation to the deposit's centerline are corrected for each deposit with regard to the measured distance from centerline to the temperature measurement points.

3. Results and discussion

3.1. Influence of process parameters

The maximum process temperatures recorded by the inserted thermocouples are used for the analysis of the influence of process parameters on the temperature. Setting the reference process parameters to 8 kN axial force, 1200 rpm rotational speed and 6 mm/s travel speed, a maximum temperature of 394.8 °C was measured by the thermocouple at a planned position 2.5 mm to the advancing side. Due to the necessary correction of the measurement positions with regard to the deposit this thermocouple results to be approximately in the center of the deposit. This shift of consumable stud and deposit to the advancing side, which is observed throughout the processes, is consistent with the observation by Sakihama et al. [26]. Fig. 3 illustrates the measured maximum temperatures along the cross-section of the deposit for varied process parameters as well as the resulting geometric dimensions of the deposit. Overall, it can be noted that the temperatures on the advancing side are slightly higher than on the retreating side, which is in agreement with other studies [16,26,27].

A reduction of the applied axial force, keeping the other process parameters constant, leads to lower maximum process temperatures. A reduction by 2 kN resulted in an approximately 20 °C lower maximum process temperature, see Fig. 3a. Accordingly, an increase in axial force leads to higher maximum process temperatures agreeing with results from former studies [16,17]. The applied axial force is one major factor determining the energy during the process. The effect of change in applied axial force on the maximum process temperatures seems to be more pronounced on the retreating side than on the advancing side.

An increased rotational speed from the reference process parameters seems to hardly influence the maximum process temperatures, see Fig. 3c. In contrast, a lower rotational speed led to decreased maximum process temperatures for the measurements close to deposition center.

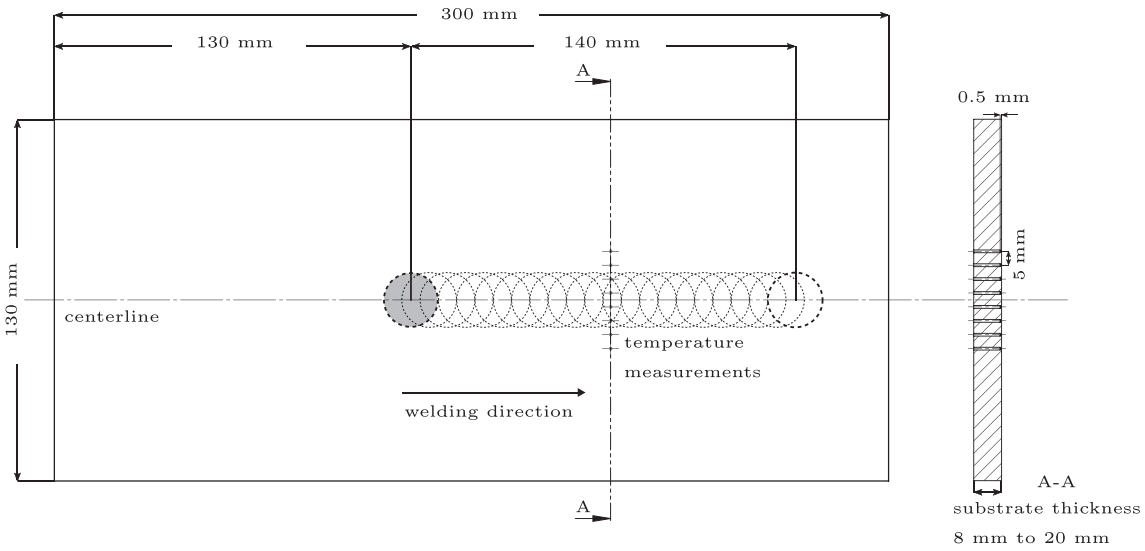

Fig. 1. Schematic positioning of consumable stud (125 mm length, 20 mm diameter) and welding path in relation to temperature measurement positions (drilled holes for the thermocouples in substrate plate).

Former studies showed higher temperatures as rotational speed is increased for FS of aluminum [16,17] as well as for titanium [28]. For the presented results, the effect of rotational speed on the maximum process temperatures seems to be much more localized compared to the results for varying the axial force, so that the outer measurement points did not show significant difference in maximum temperature for the different rotational speeds. Still, the rotational speed is one main factor determining the energy that is put into the process.

A reduction of the travel speed leads to higher maximum temperatures at all measurement positions compared to the reference process conditions, see Fig. 3e. The maximum temperature increased by around 50 °C as the travel speed is decreased by 2 mm/s. In contrast, an increase in travel speed by 2 mm/s did not show a considerable change in the maximum process temperatures compared to the reference travel speed of 6 mm/s. Since the travel speed determines the process duration, the heat is applied over a longer period of time leading typically to higher temperatures when decreased travel speeds are applied. However, no decrease in temperature could be observed for increased travel speed. Therefore, it can be assumed that the process temperatures are minimal for the reference travel speed of 6 mm/s and a further increase does not have a significant effect on process temperature measured in the substrate.

Next to the maximum process temperatures, the geometric dimensions of the deposit are shown in Fig. 3. The deposit width and thickness for the varied axial force are illustrated in Fig. 3b. Thinner and wider deposits are observed for increased forces. Higher rotational or travel speeds lead to reduction in deposit thickness and width, see Fig. 3d and f. The deposit thickness and width are decreased for increased travel speeds. The observed deposit thickness and width for the varied process parameters confirm the relation between process parameters and deposit geometry as documented by numerous studies discussed in the review articles [10,29].

3.2. Influence of substrate thickness and process environment

For the investigation of the effect of substrate thickness and process environment, i.e. studholder and backing plate material, on the maximum process temperature, the process parameters were kept constant at the reference process parameters of 8 kN applied axial force, 1200 rpm rotational speed and 6 mm/s travel speed. The maximum process temperatures for varied substrate thickness are shown in Fig. 4a. The maximum temperature values are significantly lower for a 12 mm substrate than for an 8 mm substrate, however, a further increase in substrate thickness does not lead to significant changes in maximum process temperature. Compared to thin substrates of 8 mm, it can be assumed that the heat profile over substrate depth is altered when a thicker substrate of 12 mm is used. This results in lower maximum process temperatures. At a certain thickness the heat dissipation to the substrate material is maximal and further increase of substrate thickness does not have a further effect on process temperature. This is consistently observed for an Al as well as for a Ti backing plate, see Fig. 4a, c. The maximum process temperatures are higher when the Ti

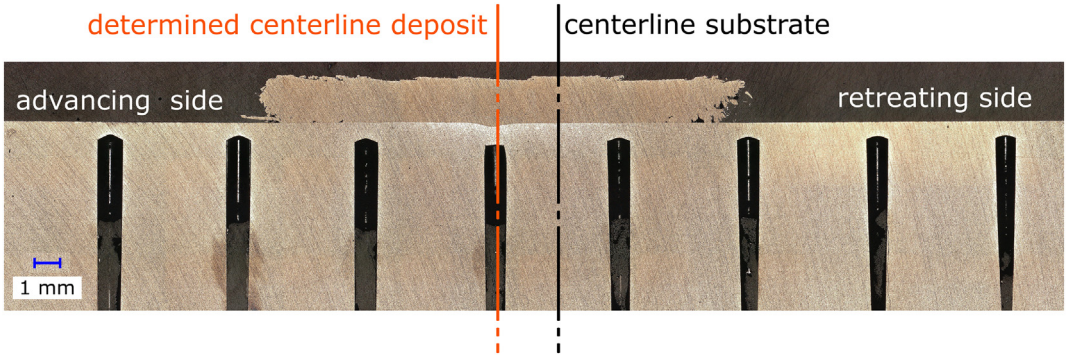

Fig. 2. Macrograph of the substrate with holes for temperature measurements and layer deposited at process parameters 8 kN, 1200 rpm and 6 mm/s. Determined centerline of the deposit does not correspond to the centerline of the substrate.

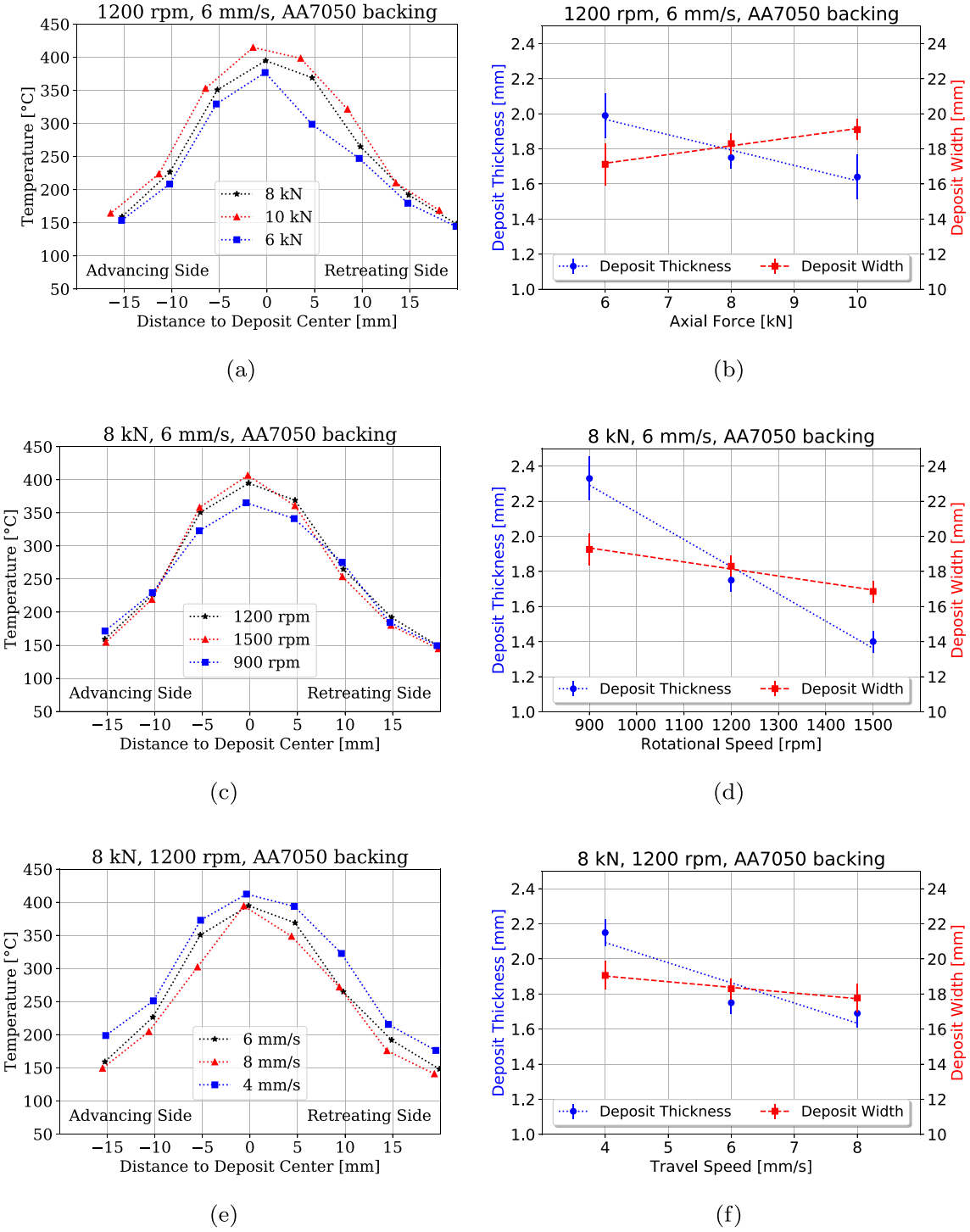

Fig. 3. Maximum process temperature at the eight measurement points and deposit geometry, as exemplarily shown in Fig. 2, in AA 7050 substrate (130 mm × 300 mm × 10 mm) with AA 7050 backing (130 mm × 300 mm × 8 mm) for variation of force (a) and (b), rotational speed (c) and (d), and travel speed (e) and (f). The deposit center is corrected based on the optical macrographs of each experiment in order to correspond with the real center of the deposit.

backing plate is used. The lower thermal conductivity of titanium leads to higher temperatures in the substrate since the heat cannot conduct as easy from substrate into the backing as it is the case when an aluminum backing is used.

The trends in deposit geometry for varied substrate thickness are shown in Fig. 4b, d. The thicker the substrate, the higher is the deposit thickness for constant process parameters. For instance, in comparison to the 8 mm substrate, an increase in thickness of 0.4 mm or 0.7 mm is observed for the 20 mm substrate, with Al or Ti backing, respectively. The deposit width tends to be constant or minimal lower, the thicker the substrate. Also, the deposits are thinner and minimal wider when a Ti backing plate is used.

Fig. 5 shows the maximum process temperatures for different studholder and backing materials at the reference process parameters. Comparing the results for both studholder materials, either for Al or Ti backing, see Fig. 5a, c, the temperature distributions are similar, but the results for the Al studholder indicate a shift of the temperature distribution to the retreating side, i.e. the temperatures tend to be lower on

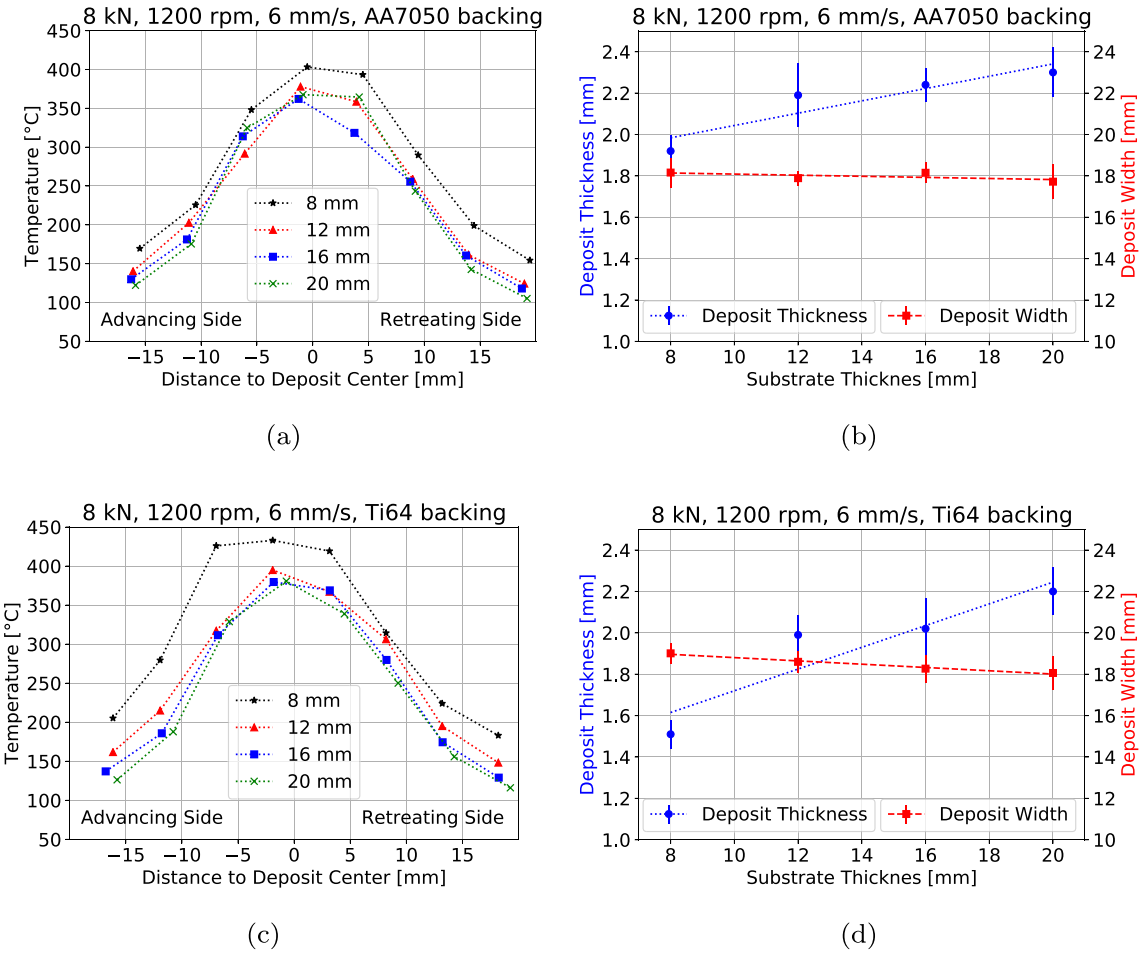

Fig. 4. Maximum process temperature at the eight measurement points and deposit geometry, as exemplarily shown in Fig. 2, in AA7050 substrate (130 mm, 300 mm, varied thickness 8 mm to 20 mm) with Al backing plate (a), (b) or Ti backing plate (c), (d).

the advancing side and higher on the retreating side compared to the distribution obtained for the X 37 studholder. Since the precise position of the measurement positions in relation to the resulting deposit is approximated, this is an uncertainty, which has to be considered when interpreting the presented results. The effect of the studholder material is more pronounced in combination with the Al backing plate. This might be related to the better heat conductivity of Al compared to Ti, increasing the effect of the higher heat conductivity of the studholder as well. Since more a shift of the temperature distribution rather than a change of the maximum process temperature is observed, a change of the studholder material does not have a notable effect on the deposit thickness and width, see Fig. 5b, d.

In summary, the thermal properties of the entire FS system, including substrate thickness and backing material, influence the process temperatures, which determine the resulting deposit geometry as discussed in the following section.

3.3. Correlation between process temperature and deposit geometry

The presented results illustrate in detail how the temperature changes depending on process parameters, substrate thickness and process environment, underlining the complexity of relevant parameters in the FS process. The differences in terms of temperature are either resulting from a change of the energy input via process parameter variations, or a change in the heat conduction conditions of the FS system, e.g. due to different substrate thicknesses or backing plate materials. For the process variations investigated in this study, the maximum difference in temperature was about 71 °C. But not only the temperature is affected by varied process conditions, but also deposit geometry, i.e. thickness and width, are significantly influenced. The previously presented results clearly illustrate that not only a change in process parameters but also changes in substrate thickness and process environment led to significant changes in the deposit geometry. This finding clearly indicates that the process temperature is an important factor for the resulting deposit geometry.

Consequently, the deposit thickness and width are displayed over the maximum temperatures obtained under the different process conditions, see Fig. 6. The deposit thickness tends to be reduced when higher process temperatures are reached during the deposition process. Furthermore, the deposit width increases for higher maximum process temperatures. The temperature can be increased either by an increased energy input, e.g. increase in axial force, or due to slower heat conduction, e.g. by changing to a backing plate of low heat conductivity. With regard to the deposition mechanism, it is assumed that there is a larger volume of plasticized material between stud and substrate present for increased process temperatures. When a larger zone of consumable material is plasticized, a higher amount of material is pressed to the outside during the process. Therefore, thinner and wider deposits are formed. This effect is facilitated when high axial forces are applied. Finally, the FS process output, the deposit, is controllable by the process temperature. Based on the presented results, it can be clearly stated that the temperature is the crucial factor for the behavior of the deposition and the material flow, determining the geometry of the resulting deposit. In summary, by adapting the process parameters, process environment and substrate thickness, the process temperatures are controlled, which determine the resulting deposit geometry.

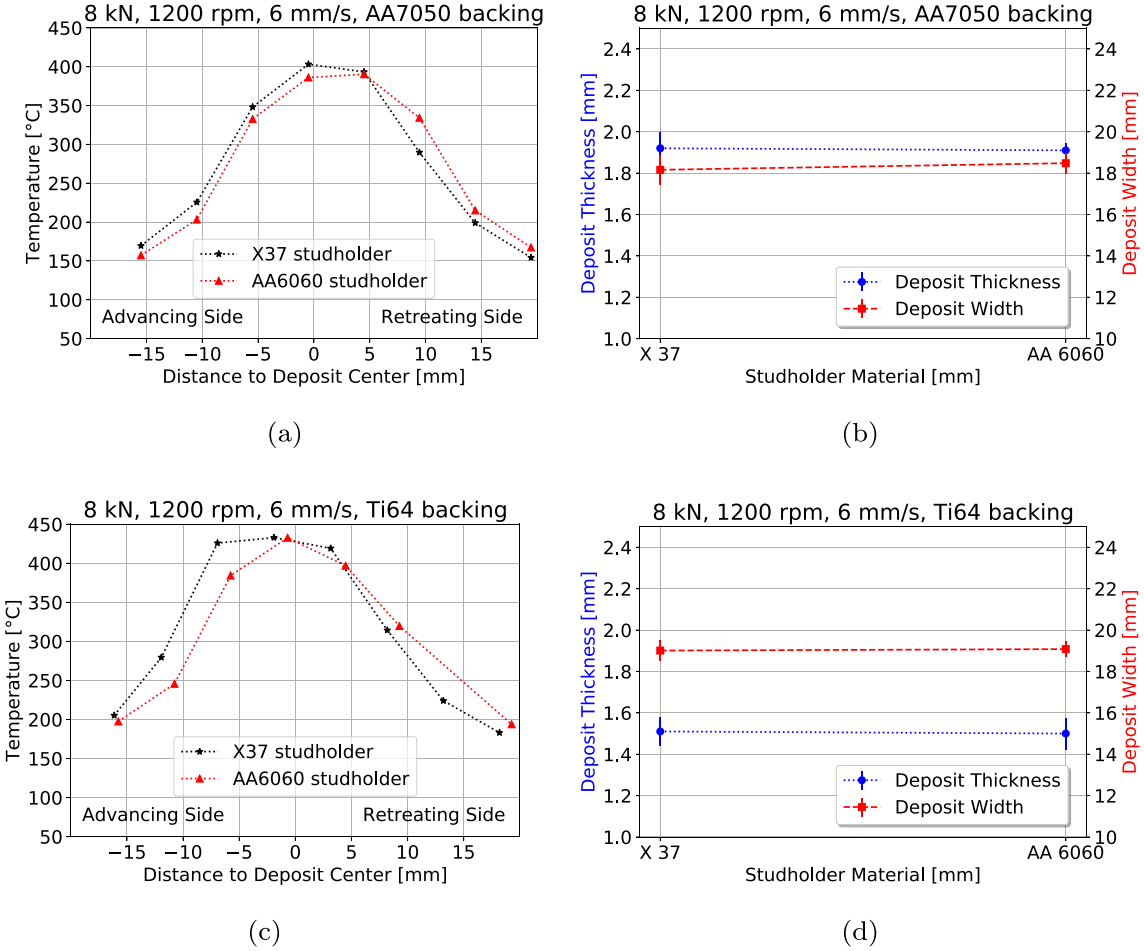

Fig. 5. Maximum temperature at the eight measurement points and deposit geometry, as exemplarily shown in Fig. 2, in AA7050 substrate (130 mm, 300 mm, 10 mm); the studholder material was AA6060 or X 37 with Al backing plate (a), (b) or Ti backing plate (c), (d).

4. Conclusion

The current study presents a detailed experimental analysis of the FS process in terms of process temperature and deposit geometry. The investigation was performed for varied process parameters and changes in substrate thickness as well as process environment. Their influence on process temperature and deposit geometry can be summarized as follows:

1. Maximum process temperature is found to be in direct (linear) relation with the deposit geometry. An increased process temperature leads to thinner and wider deposits.
2. An increase in axial process force results in higher process temperatures. The deposit is thinner and wider.
3. A decreased rotational speed leads to a decreased process temperature in the center of the weld. The deposits are thicker and wider.

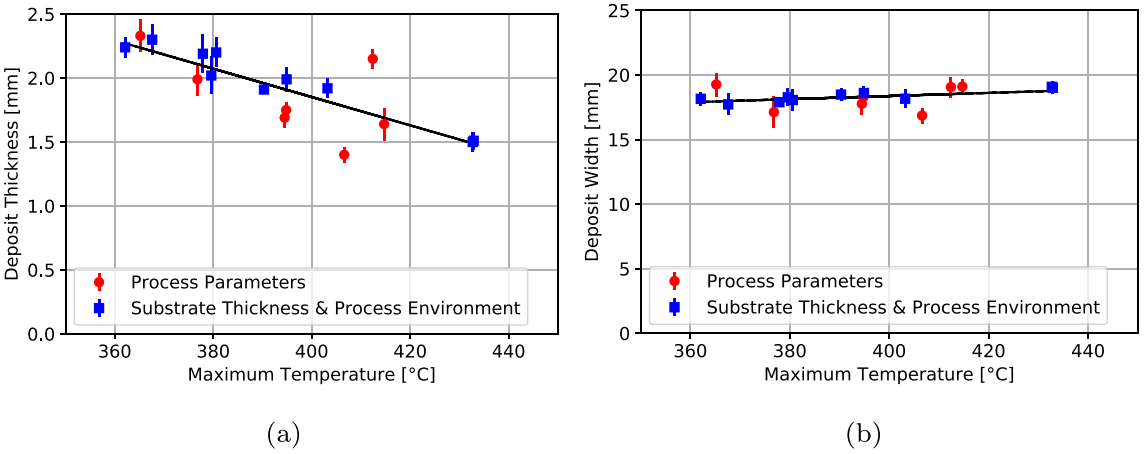

Fig. 6. The correlation of deposit geometry and maximum temperature during FS process shows that the deposit tends to be thinner and slightly wider for higher process temperatures. This is observed for process temperature changes due to change in process parameters, substrate thickness and process environment.

4. A decreased travel speed drives increased process temperatures as well as deposit width and thickness.
5. Compared to an Al backing, a Ti backing can lead to increased maximum process temperatures, resulting in thinner and wider deposits.
6. An increased substrate thickness can lead to lower process temperatures, resulting in thicker deposits of reduced width.

Funding

This research did not receive any specific grant from funding agencies in the public, commercial, or not-for-profit sectors.

CRediT authorship contribution statement

Zina Kallien: Conceptualization, Investigation, Data curation, Writing - original draft, Writing - review & editing, Visualization.**Lars Rath:**Conceptualization, Investigation, Writing - review & editing.**Arne Roos:**Writing - review & editing, Supervision.**Benjamin Klusemann:**Conceptualization, Resources, Writing - review & editing, Supervision.

Declaration of competing interest

The authors declare that they have no known competing financial interests or personal relationships that could have appeared to influence the work reported in this paper.

References

[1] R.M. Miranda, J.P. Gandra, P. Vilaca, L. Quintino, T.G. Santos, Surface Modification by Solid State Processing, Woodhead Publishing in mechanical engineering, Elsevier Science, Burlington, 2013.
[2] M.L. Kramer de Macedo, G.A. Pinheiro, J.F. dos Santos, T.R. Strohaecker, Deposit by friction surfacing and its applications, Weld. Int. 24 (6) (2010) 422–431.
[3] J. Gandra, R.M. Miranda, P. Vilaça, Performance analysis of friction surfacing, J. Mater. Process. Technol. 212 (8) (2012) 1676–1686.
[4] V.I. Vitanov, I.I. Voutchkov, Process parameters selection for friction surfacing applications using intelligent decision support, J. Mater. Process. Technol. 159 (1) (2005) 27–32.
[5] J.J.S. Dilip, G.D. Janaki Ram, B.E. Strucker, Additive manufacturing with friction welding and friction deposition processes, Int. J. Rapid Manuf. 3 (1) (2012) 56–69.
[6] J.J.S. Dilip, S. Babu, S.V. Rajan, K.H. Rafi, G.D. Janaki Ram, B.E. Stucker, Use of friction surfacing for additive manufacturing, Mater. Manuf. Process. 28 (2) (2013) 189–194.
[7] J. Shen, S. Hanke, A. Roos, J.F. Dos Santos, B. Klusemann, Fundamental study on additive manufacturing of aluminium alloys by friction surfacing layer deposition, AIP Conference Proceedings 2113 (2019) 10015.
[8] Y. Yamashita, K. Fujita, Newly developed repairs on welded area of lwr stainless steel by friction surfacing: technical report, J. Nucl. Sci. Technol. 38 (10) (2001) 896–900.
[9] Y. Huang, Z. Lv, L. Wan, J. Shen, J.F. dos Santos, A new method of hybrid friction stir welding assisted by friction surfacing for joining dissimilar Ti/Al alloy, Mater. Lett. 207 (2017) 172–175.
[10] J. Gandra, H. Krohn, R.M. Miranda, P. Vilaça, L. Quintino, J.F. Dos Santos, Friction surfacing—a review, J. Mater. Process. Technol. 214 (5) (2014) 1062–1093.
[11] J.C. Galvis, P. Oliveira, M.F. Hupalo, J.P. Martins, A. Carvalho, Influence of friction surfacing process parameters to deposit AA6351-T6 over AA5052-H32 using conventional milling machine, J. Mater. Process. Technol. 245 (2017) 91–105.
[12] H. Khalid Rafi, G.D. Janaki Ram, G. Phanikumar, K. Prasad Rao, Friction surfaced tool steel (h13) coatings on low carbon steel: a study on the effects of process parameters on coating characteristics and integrity, Surf. Coat. Technol. 205 (1) (2010) 232–242.
[13] H. Khalid Rafi, G.D.J. Ram, G. Phanikumar, K.P. Rao, Friction surfacing of austenitic stainless steel on low carbon steel: studies on the effects of traverse speed, Proceedings of the World Congress on Engineering, 2 2010.
[14] D. Govardhan, K. Sammaiah, K. Murti, G.M. Reddy, Evaluation of bond quality for stainless steel-carbon steel friction surfaced deposits, Mater. Today: Proceedings 2 (2015) 3511–3519.
[15] S. Hanke, P. Staron, T. Fischer, V. Fitseva, J.F. Dos Santos, A method for the in-situ study of solid-state joining techniques using synchrotron radiation - observation of phase transformations in Ti-6Al-4V after friction surfacing, Surf. Coat. Technol. 335 (2017) 355–367.
[16] P. Pirhayati, H. Jamshidi Aval, An investigation on thermo-mechanical and microstructural issues in friction surfacing of Al–Cu aluminum alloys, Mater. Res. Express 6 (5) (2019) 056550.
[17] Z. Rahmati, H. Jamshidi Aval, S. Nourouzi, R. Jamaati, Modeling and experimental study of friction surfacing of aa2024 alloy over aa1050 plates, Mater. Res. Express 6 (8) (2019) 0865g2.
[18] X.M. Liu, Z.D. Zou, Y.H. Zhang, S.Y. Qu, X.H. Wang, Transferring mechanism of the coating rod in friction surfacing, Surf. Coat. Technol. 202 (9) (2008) 1889–1894.
[19] H. Khalid Rafi, K. Balasubramaniam, G. Phanikumar, K. Prasad Rao, Thermal profiling using infrared thermography in friction surfacing, Metall. Mater. Trans. A 42 (11) (2011) 3425–3429.
[20] W. Tang, X. Guo, J.C. McClure, L.E. Murr, A. Nunes, Heat input and temperature distribution in friction stir welding, J. Mater. Process. Manuf. Sci. 7 (1998) 163–172.
[21] S. Hanke, J.F. Dos Santos, Comparative study of severe plastic deformation at elevated temperatures of two aluminium alloys during friction surfacing, J. Mater. Process. Technol. 247 (2017) 257–267.
[22] U. Suhuddin, S. Mironov, H. Krohn, M. Beyer, J.F. Dos Santos, Microstructural evolution during friction surfacing of dissimilar aluminum alloys, Metall. Mater. Trans. A 43 (13) (2012) 5224–5231.
[23] J. Ehrich, A. Roos, S. Hanke, Effect of Mg and Si content in aluminum alloys on friction surfacing processing behavior, in: C. Chesonis (Ed.), Light Metals 2019, Springer International Publishing, 2019, pp. 357–363.
[24] H. Krohn, S. Hanke, M. Beyer, J.F. Dos Santos, Influence of external cooling configuration on friction surfacing of AA6082 T6 over AA2024 T351, Manuf. Lett. 5 (2015) 17–20.
[25] F.Y. Isupov, O. Panchenko, L. Zhabrev, I. Mushnikov, E. Rylkov, A.A. Popovich, Finite element simulation of temperature field during friction surfacing of Al-5Mg consumable rod, Key Eng. Mater. 822 (2019) 737–744.
[26] H. Sakihama, H. Tokisue, K. Katoh, Mechanical properties of friction surfaced 5052 aluminum alloy, Mater. Trans. 44 (12) (2003) 2688–2694.
[27] K. Badheka, V. Badheka, Friction surfacing of aluminium on steel: an experimental approach, Mater. Today: Proceedings 4 (9) (2017) 9937–9941.
[28] V. Fitseva, S. Hanke, J.F. Dos Santos, Influence of rotational speed on process characteristics, material flow and microstructure evolution in friction surfacing of ti-6al-4v, Mater. Manuf. Process. 32 (5) (2016) 557–563.
[29] S. Mohanasundaram, S.J. Vijay, M. Karthikeyan, A review on developing surface composites using friction surfacing, Appl. Mech. Mater. 852 (2016) 402–410.